

A multicritical point of $S = 1$ XXZ chain with single ion anisotropy

Shuichi Shiraishi* and Kiyohide Nomura†
*Department of Physics, Kyushu University,
 Fukuoka 819-0395, Japan*

(Dated: October 7, 2024)

We research the ground state of the $S = 1$ XXZ spin chain with single ion anisotropy, focusing on XY1, XY2 (Spin Nematic), Néel, Haldane phases. Recently, it was reported that the four phases did not intersect at a single point using conventional numerical methods, which is inconsistent with the bosonization theory. In order to resolve this discrepancy, we propose a unified method to determine phase boundaries by combining conformal field theory (CFT) with numerical diagonalization. And we discuss the symmetry and universality class of the multicritical point.

I. INTRODUCTION

$S = 1$ XXZ spin chain with single ion anisotropy, which is given by

$$H = \sum_j (S_j^x S_{j+1}^x + S_j^y S_{j+1}^y + \Delta S_j^z S_{j+1}^z + D(S_j^z)^2) \quad (1)$$

has been studied by many authors and especially, in detail by Schulz [1] and Chen, Hida, Sanctuary [2]. According to their studies, the model has several different phases in the ground state depending on the Hamiltonian parameters. In particular, there are regions where four phases, called the XY1, XY2, Haldane, and Néel phases, are adjacent to each other.

At first we overview phases of model (1). Ferromagnetic phase is characterized with the ferromagnetic long-range order, and Néel phase with the Néel long-range order. On the other hand, there is no long-range order in the Haldane, large D , XY1 and XY2 phases. The correlation lengths are finite in the Haldane and the large D phases, though correlation lengths diverge in the XY1 and XY2 phases (or massless phases). Universality class of the XY1-Haldane and the XY1-large D phase transition belongs to the Berezinskii-Kosterlitz-Thouless (BKT) transition type, and the Haldane-large D phase transition belongs to the Gaussian fixed line associated with BKT transition.

In Schulz's work, analytical methods applying bosonization were used, while the work of Chen et al. was well investigated numerically. However, Chen et al. used two different methods for Néel-Haldane phase boundary and for XY1-XY2. This is because the method for an order-disorder transition is inappropriate for determining the XY1-XY2 phase boundary. In this case, recent numerical study [10] suggested that the four phases did not intersect at a single point, a result that is inconsistent with Schulz's work. By the way, since the model (1) has

two parameters Δ and D , the phase boundary between two phases is a line, the phase boundary between three phases is a point. But for four phases, there is not intersection in general. Thus, we should check the Schulz's statement.

The main purpose of this study is to investigate the physics around this multiple critical point using a unified method, and we discuss the critical phenomena by obtaining the energy with numerical diagonalization and conformal field theory.

Using the method described in Section 3, we obtain a phase diagram in FIG. 1. Here the XY1-Haldane and the XY2-Néel boundaries are on the $\Delta = 0$ line. The Haldane-Néel and XY1-XY2 phase boundaries are connected smoothly, and four phases intersect at the tetracritical point $\Delta = 0, D = -2.0351 \pm 0.0034$.

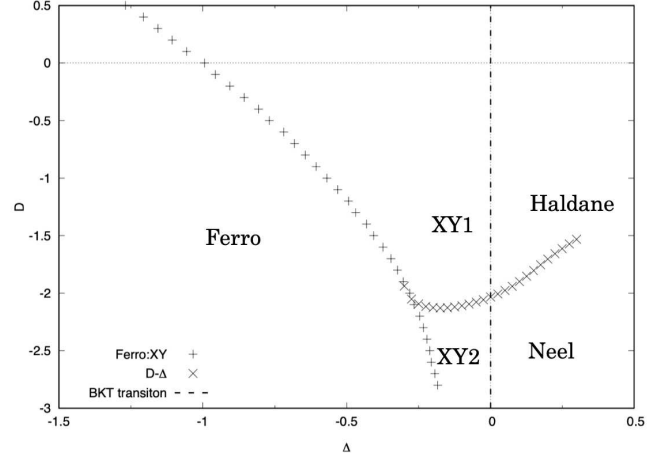


FIG. 1. Phase diagram : Haldane-Néel and the XY1- XY2 phase boundaries are connected continuously and four phases intersect as the tetracritical point.

Note that the line of $\Delta = 0$ is BKT transition. This is supported by using the special $SU(2)$ symmetry argument in the work of Kitazawa, Hijii, and Nomura [3]. According to their study, in addition to the $SU(2)$ symmetry of the conventional spin operators, there exists a

* s.shiraishi@stat.phys.kyushu-u.ac.jp

† knomura@stat.phys.kyushu-u.ac.jp

special SU(2) symmetry based on relations as below,

$$[S_j^z, (S_k^\pm)^2] = \pm 2\delta_{jk}(S_j^\pm)^2 \quad (2)$$

and

$$[(S_j^+)^2, (S_k^-)^2] = 4\delta_{jk}S_j^z. \quad (3)$$

In addition, when $\Delta = 0$, the Hamiltonian (1) and $\sum_k (S_k^\pm)^2$ commute.

One of the authors proposed the level spectroscopy technique [4, 5] to treat BKT transition, by combining renormalization group, symmetry and numerical data. For the Gaussian fixed line, Kitazawa proposed the twist boundary method [6]. However, the distinction between the XY1 and XY2 phases is subtle, which we will explain in the following sections.

We review a short history of the XY1 and XY2 phases. By using perturbation and numerical diagonalization, Solyom and Ziman [7] studied S=1 XXZ spin chain with single ion anisotropy and discussed the planar phase, but they did not distinguish the two (XY1-XY2) phases.

Later, combining numerical diagonalization and bosonization, Schulz and Ziman [8] discussed there are two phases in massless phases; planar1 (XY1) and planar2 (XY2). Schulz [1] explained the bosonization technique for the XXZ chain with single ion anisotropy for general spin S cases, where he expressed spin S chain by the spin ladder with ferromagnetic rung couplings, and then studied two continuous effective field models. One effective field model induces the BKT transition, and another induces the 2D Ising type transition, thus there appear four phases.

Chen et al.[2] studied the S=1 XXZ spin chain with single ion anisotropy, using numerical diagonalization and the level spectroscopy technique [5], and they found that the BKT transition line (XY1-Haldane and XY2-Néel) is located just on the $\Delta = 0$. They also determined the large D-Haldane phase boundary, by using the twist boundary method.

However, since they used the different methods to determine the Haldane-Néel phase boundary (phenomenological renormalization group method; PRG[9]) and the XY1-XY2 phase boundary, thus these two phase boundaries may not connect continuously for finite system. In fact, recently, Tonegawa et al.[10] studied S=1/2 ferromagnetic-antiferromagnetic bond-alternating chain, which is considered to belong to the same universality type as S=1 XXZ chain with single ion anisotropy, by analyzing numerical diagonalization. Especially in the four phases, that is, spin nematic Tomonaga-Luttinger (nTLL), up-up-down-down (UUDD), singlet-dimer (SD) phases, where nTLL phase corresponds to XY2 phase, UUDD to Néel, SD to Haldane, they found several tricritical points. We consider that such tricritical points may be artificial one coming from different numerical methods, thus we propose a new unified method to determine the XY1-XY2 phase boundary and the Haldane-Néel phase boundary.

Let us mention one model which shows such a tetra-critical behavior; the bilinear-biquadratic (BLBQ) model with single ion anisotropy

$$H = \sum_j (\cos\theta(\mathbf{S}_j \cdot \mathbf{S}_{j+1}) + \sin\theta(\mathbf{S}_j \cdot \mathbf{S}_{j+1})^2) + D \sum_j (S_j^z)^2. \quad (4)$$

At the Takhtajan-Babujian (TB) point $D = 0$ and $\theta = \pi/4$, this model is Bethe-Ansatz solvable [11, 12]. Field theoretical models at this point were proposed by [13] and [14]. Numerically, it was found that the four phases (Haldane, dimer, Néel, large D) meet at the TB point [15, 16]. Then, the following question arises: whether the universality class of the tetracritical point of model (1) is the same with that of the TB point or not?

In Sec.II, we summarize Schulz's discussion. In Sec.III, we carry out numerical calculations, and propose a new method. In Sec.IV, we discuss symmetry aspects of this model (1). In Sec.V, the conclusions of this paper are shown. In the Appendix, we overview the effective Hamiltonian based on the perturbation calculations.

II. REVIEW OF SCHULZ'S DISCUSSION

Schulz pointed out in reference [1] that there are two different types of XY phases with different characteristics. First, the XY1 and XY2 phases are characterized by the following spin correlation functions, which show both a power-law decay and an exponential decay respectively. In XY1 phase, they are

$$\begin{aligned} \langle S_j^+ S_{j+r}^- \rangle &\propto (-1)^r r^{-\eta_1} \\ \langle (S_j^+ S_j^+) (S_{j+r}^- S_{j+r}^-) \rangle &\propto r^{-\eta_2} \\ \langle S_j^z S_{j+r}^z \rangle &= C_z r^{-2} + D_z (-1)^r \exp(-r/\xi_z) \end{aligned} \quad (5)$$

where, $0 < \eta_1 < 1/4$ and $\eta_2 = 4\eta_1$. Then, on the boundary of XY1-Haldane, they are $\eta_1 = 1/4$, $\eta_2 = 1$.

In XY2 phase,

$$\begin{aligned} \langle S_j^+ S_{j+r}^- \rangle &\propto (-1)^r \exp(-r/\xi_1) \\ \langle (S_j^+ S_j^+) (S_{j+r}^- S_{j+r}^-) \rangle &\propto r^{-\eta_2} \\ \langle S_j^z S_{j+r}^z \rangle &\propto (-1)^r r^{-\eta_z} \end{aligned} \quad (6)$$

where $0 < \eta_2 < 1$, $\eta_z = 1/\eta_2$, and on the boundary of XY2-Néel, $\eta_2 = 1$.

Furthermore, correlation functions are in Haldane phase,

$$\begin{aligned} \langle S_j^+ S_{j+r}^- \rangle &\propto (-1)^r \exp(-r/\xi_1) \\ \langle (S_j^+ S_j^+) (S_{j+r}^- S_{j+r}^-) \rangle &\propto \exp(-r/\xi_2) \\ \langle S_j^z S_{j+r}^z \rangle &\propto (-1)^r \exp(-r/\xi_z), \end{aligned} \quad (7)$$

whereas in Néel phase,

$$\begin{aligned} \langle \hat{S}_j^+ \hat{S}_{j+r}^- \rangle &\propto (-1)^r \exp(-r/\xi_1) \\ \langle (\hat{S}_j^+ \hat{S}_j^+) (\hat{S}_{j+r}^- \hat{S}_{j+r}^-) \rangle &\propto \exp(-r/\xi_2) \\ \langle \hat{S}_j^z \hat{S}_{j+r}^z \rangle &\propto (-1)^r. \end{aligned} \quad (8)$$

From the lattice model (1), Schulz deduced two independent field models. One field model induces the BKT transition, whereas another induces the 2D Ising type transition. Therefore he concluded the four phases (XY1, XY2, Haldane, Néel) intersect at one point.

By the way, in the conformal field theory (CFT) language, the XY1 and the XY2 phases belong to the central charge $c = 1$. The Haldane-Néel phase boundary belongs to the $c = 1/2$ CFT (or 2D Ising type universality). For a review of conformal field theory, reference [17] is helpful.

Finally, with perturbative calculations in $D \rightarrow -\infty$ limit as described in appendix, one can obtain an effective model which has the ferromagnetic, XY2 and Néel phases. This is consistent with the above mentioned Schulz's discussion.

III. NUMERICAL ANALYSIS

In this section, we show the numerical analysis. The energy of system is calculated by numerical diagonalization. Considering dispersion relation, we define wave number as

$$q = \frac{2\pi}{L}n, \quad (9)$$

and spin wave velocity as

$$v_0 = \left. \frac{dE(q)}{dq} \right|_{q=0}, \quad (10)$$

magnetization as the sum of the z component spins,

$$m = \sum_j S_j^z \quad (11)$$

as follows. Where, n is integer and $E(q)$ is the energy at magnetization $m = 0$ and wavenumber q . And also, we define the translation operator \hat{T} as acting like

$$\hat{T}^\dagger \hat{S}_j \hat{T} = \hat{S}_{j+1} \quad (12)$$

so that under periodic boundary conditions,

$$\begin{aligned} \hat{T}^L |phys\rangle &= \hat{T}^{L-1} \hat{T} |phys\rangle \\ &= \hat{T}^{L-1} e^{iq} |phys\rangle \\ &= e^{iq} \hat{T}^{L-1} |phys\rangle \\ &= e^{iqL} |phys\rangle \\ &= |phys\rangle \end{aligned} \quad (13)$$

where L is the number of sites and $|phys\rangle$ denotes the eigenstates of \hat{T} .

Now, since the spin wave velocity is defined by the derivative, ground state energy E_g and v_0 can be specifically calculated numerically by replacing and treating it as the difference

$$v_0(L) = \frac{E(q = 2\pi/L) - E(q = 0)}{2\pi/L} \quad (14)$$

A. Effective central charge

Previous numerical studies have shown that the central charge $c = 1$ in XY1 [18] and $c = 1$ in XY2 phase [2](see also appendix). In this subsection, we would like to confirm this fact and investigate the central charge at the phase boundaries. Here we take the approach of confirming the singularity by analyzing how the central charge c depends on D , which is an anisotropic parameter. First, it is known that when conformal field theory holds,

$$\frac{E_g(L)}{L} = \epsilon_\infty - \frac{\pi v_0 c}{6L^2}, \quad \frac{E_g(L-2)}{L-2} = \epsilon_\infty - \frac{\pi v_0 c}{6(L-2)^2} \quad (15)$$

from the discussion on finite size scaling, [19] [20] where E_g is the ground state energy, L is the system size, and ϵ_∞ is the ground energy per unit site in the thermodynamic limit.

Considering the difference in equation (15), we can get the relation

$$\begin{aligned} c(L, L-2) &= \left\{ \frac{E_g(L)}{L} - \frac{E_g(L-2)}{L-2} \right\} \\ &\times \left\{ -\frac{\pi}{6} \left(\frac{v_0(L)}{L^2} - \frac{v_0(L-2)}{(L-2)^2} \right) \right\}^{-1}. \end{aligned} \quad (16)$$

Thus, $c(L, L-2)$ can be obtained by numerical data $E_g(L)$ and $v_0(L)$, and we shall call it as the effective central charge.

FIG. 2 plots the curves for each system size L , with D on the horizontal axis and the central charge $c(L)$ on the vertical axis. The results of numerical calculations using the exact diagonalization method are used for the bottom energies for system sizes $L = 8, 10, 12, 14, 16$ and 18 . The results of extrapolation to obtain the value of D when c takes a peak and the value of c at that time are shown in FIG. 3 and FIG. 4. Here we extrapolated the effective central charge as

$$c_{peak}(L-1) = c_{peak}(\infty) + \alpha_1 \frac{1}{(L-1)^2} + \alpha_2 \frac{1}{(L-1)^4}, \quad (17)$$

and also extrapolated D as $D_{peak}(L-1) = D_{peak}(\infty) + \beta_1 \frac{1}{(L-1)^2} + \beta_2 \frac{1}{(L-1)^4}$ [21],[22].

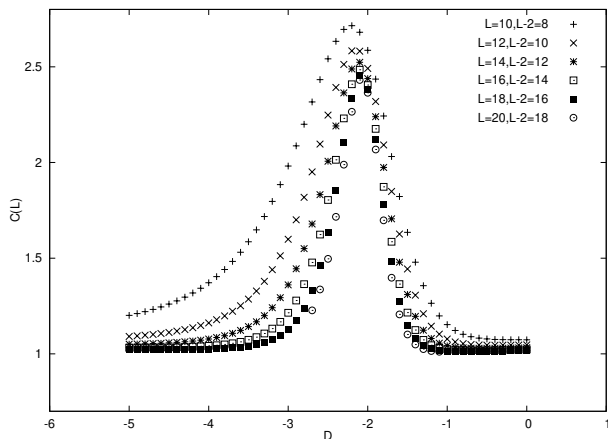


FIG. 2. Effective central charge at $\Delta = 0$: In the region $D \neq -2$, c takes the predicted value, but at the region around $D \sim -2$ it differs from the naive expectation.

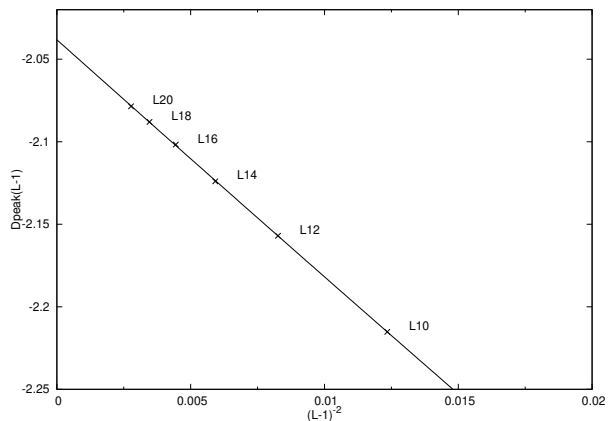


FIG. 3. The peak of D identification by central charge at $\Delta = 0$.

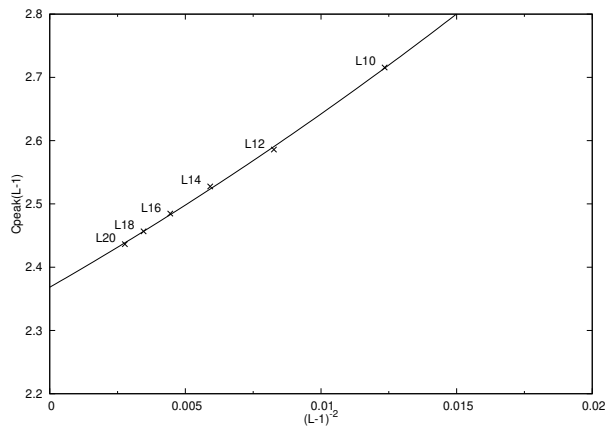


FIG. 4. The extrapolation of the peak of effective central charge at $\Delta = 0$.

From Fig. 2, we read the effective central charge becomes $c = 1$, except for $D \sim -2$. In Fig. 3, we plot the peak positions of the effective central charge as a function of size, and we extrapolate the tetracritical point $D = -2.03686, \Delta = 0$ in the infinite limit. Assuming that the central charge of one phase is c_1 , the other is c_2 , and the spin wave velocity v_0 is common at the phase boundary, the following simple prediction can be made,

$$\frac{E_g(L)}{L} = \epsilon_\infty - \frac{\pi v_0 (c_1 + c_2)}{6L^2}. \quad (18)$$

On the basis of this relationship, we may expect the central charge $c = 3/2$ at the tetracritical point, which is the sum of $c = 1$ and $c = 1/2$. For the TB point of (4), this assertion is correct, since the $c = 1/2$ line (on the Haldane-Néel and dimer-large D phase boundaries) and the $c = 1$ line (on the Haldane-large D and Néel-dimer phase boundaries) cross at the TB point with central charge $c = 3/2$ [13, 14].

In contrast, at the tetracritical point of the present model (1), the effective central charge $c = 2.368$ obtained in Fig. 2 and 4, deviates largely from $c = 3/2$. We consider that this discrepancy comes from the assumption of a unique spin wave velocity.

B. Massless case

Even in the case where multiple spin-wave velocities appear, the problem in the previous section can be avoided by using relation (19) at three system sizes, $L + 2, L, L - 2$. In other words, we consider estimating the phase boundaries by the ratios as explained below, without directly obtaining the central charge.

1. Definition of the 'ratio'

If there exist two spin wave velocities v_1 and v_2 ,

$$\frac{E_g(L)}{L} = \epsilon_\infty - \frac{\pi}{6L^2} (v_1 c_1 + v_2 c_2), \quad (19)$$

would be viable instead of (15). This relation may be written as

$$\frac{E_g(L+2)}{L+2} - \frac{E_g(L)}{L} = -\frac{\pi}{6} \left(\frac{1}{(L+2)^2} - \frac{1}{L^2} \right) (v_1 c_1 + v_2 c_2) \quad (20)$$

and

$$\frac{E_g(L)}{L} - \frac{E_g(L-2)}{L-2} = -\frac{\pi}{6} \left(\frac{1}{L^2} - \frac{1}{(L-2)^2} \right) (v_1 c_1 + v_2 c_2). \quad (21)$$

From (20),(21) , we obtain the relation

$$\left(\frac{\frac{E_g(L+2)}{L+2} - \frac{E_g(L)}{L}}{\frac{E_g(L)}{L} - \frac{E_g(L-2)}{L-2}} \right) / \left(\frac{\frac{1}{(L+2)^2} - \frac{1}{L^2}}{\frac{1}{L^2} - \frac{1}{(L-2)^2}} \right) = 1. \quad (22)$$

The relation (22) is established where conformal field theory can be applied. Therefore we can use the ratio of left hand side of (22) to identify the phase boundary. Let us call the left-hand side of eq.(22) Rt ,

$$Rt \equiv \left(\frac{\frac{E_g(L+2)}{L+2} - \frac{E_g(L)}{L}}{\frac{E_g(L)}{L} - \frac{E_g(L-2)}{L-2}} \right) / \left(\frac{\frac{1}{(L+2)^2} - \frac{1}{L^2}}{\frac{1}{L^2} - \frac{1}{(L-2)^2}} \right). \quad (23)$$

In the following, we will examine the dependence of the numerically calculated value of Rt on D .

2. D -peak shift by Δ

Next, we describe how to estimate the phase boundaries by obtaining the dependence of the value of Rt (23) on D for each Δ .

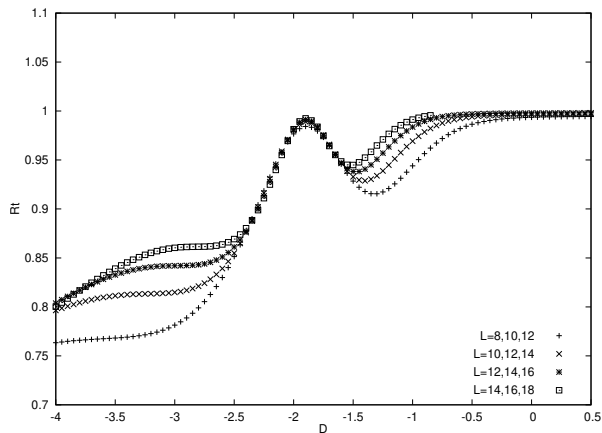


FIG. 5. Rt for each different size L are plotted, at $\Delta = 0.1$. Rt is defined by eq (21).

FIG. 5 shows the D dependence of Rt at $\Delta = 0.1$. It can be read that the value of Rt is close to 1 at $D \sim -2$. This corresponds to the Néel-Haldane boundary, which can be interpreted as a CFT with central charge $c = 1/2$. At this time, the correlation length is expected to behave,

$$\xi_z \propto |D - D_{HN}(\Delta)|^{-1}, \quad (24)$$

where ξ_z was defined in Sec.2, and $D_{HN}(\Delta)$ is a Haldane-Néel phase boundary.

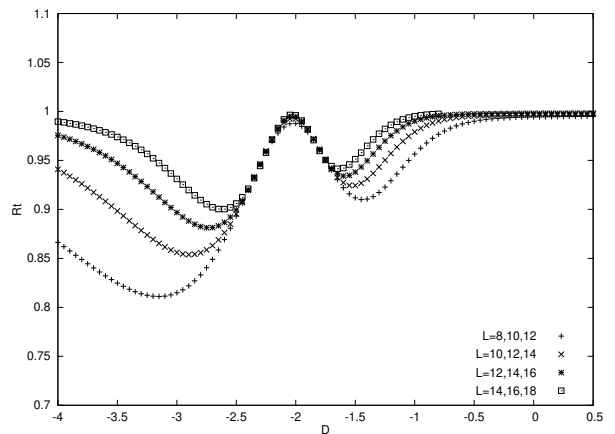


FIG. 6. $\Delta = 0$

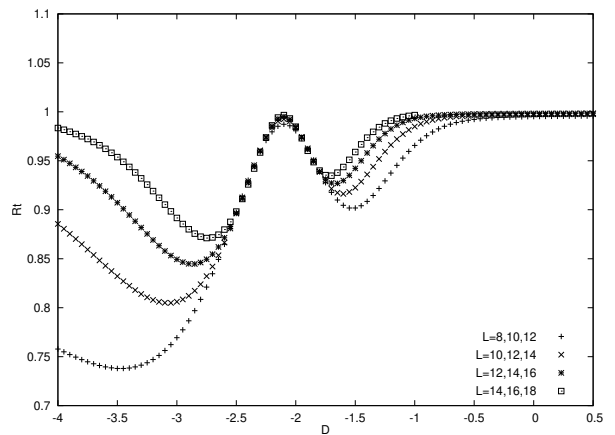


FIG. 7. $\Delta = -0.1$

Next we show the D dependence of Rt in Fig.6 ($\Delta = 0$) and Fig. 7 ($\Delta = -0.1$), respectively. Similarly, the value of Rt peaks around $D \sim -2$. From the 2D Ising universality class, at this time, the correlation lengths behave,

$$\xi_z \propto (D - D_{XY12}(\Delta))^{-1}, (XY1) \quad (25)$$

and

$$\xi_1 \propto (D_{XY12}(\Delta) - D)^{-1}, (XY2) \quad (26)$$

where ξ_z and ξ_1 were defined in Sec.2, and $D_{XY12}(\Delta)$ is a phase boundary between XY1 and XY2 phase.

As a further example, data estimated by extrapolation for the value of the peak at $\Delta = 0$ is shown in Fig.8. Here we extrapolated D as $D_{peak}(L) = D_{peak}(\infty) + \beta_1 \frac{1}{L^2} + \beta_2 \frac{1}{L^4}$ [21],[22]. We extrapolate the tetracritical point as $\Delta = 0$, $D = -2.03343$.

In summary, from the analysis such as FIG. 5-7 and FIG. 8, the Haldane-Néel phase boundary and the XY1-XY2 phase boundary are determined commonly with the peak of Rt .

The Haldane-large D phase boundary belongs to the Gaussian fixed line with central charge $c = 1$. The Gaussian fixed line associated with BKT lines form a multicritical point, and renormalization flows become very slow or extremely large ξ in the neighborhood of this BKT multicritical point, which explains the peculiar behavior of Rt in the Haldane phase close to XY1 and large D phases in Fig.5. Although it is difficult to determine the BKT transition lines and the Gaussian fixed line with the present method, it is valid to apply the level spectroscopy [3],[4] for the BKT transitions, and the Kitazawa's twisted boundary method [6] for the Gaussian fixed line. By using these methods, Haldane, large D and XY1 phase boundaries were obtained by Chen et. al.[2]. Thus in this paper we concentrate on the XY1-XY2 and Haldane-Néel phase boundaries.

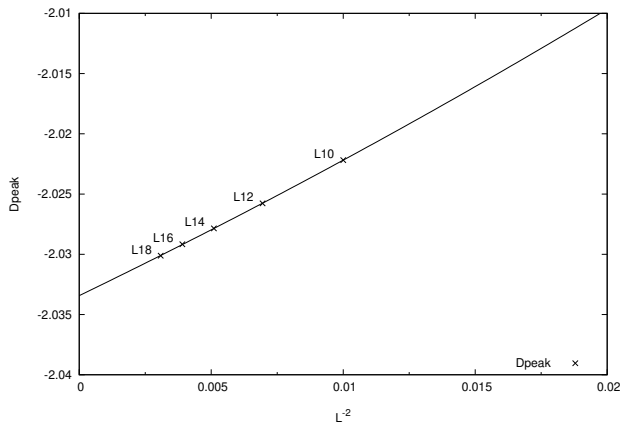


FIG. 8. The extrapolation of the D 's peak at $\Delta = 0$ for each set of different sizes $(L = 8, 10, 12), (L = 10, 12, 14), (L = 12, 14, 16), (L = 14, 16, 18), (L = 16, 18, 20)$.

C. Mixed case of finite and infinite correlation lengths

Next let us consider the mixed case that one correlation length ξ is finite, and another correlation length is infinite. The relationship assumed in this case is

$$\frac{E_g(L)}{L} = \epsilon_\infty - \frac{\pi v c}{6L^2} - k e^{-L/\xi}, \quad (27)$$

where k is a proportionality constant.

Using different sizes L ,

$$\begin{aligned} \frac{E_g(L+2)}{L+2} - \frac{E_g(L)}{L} &= -\frac{\pi}{6} \left(\frac{1}{(L+2)^2} - \frac{1}{L^2} \right) v c \\ &\quad - k (e^{-(L+2)/\xi} - e^{-L/\xi}) \\ &= -\frac{\pi}{6} \left(\frac{1}{(L+2)^2} - \frac{1}{L^2} \right) v c \\ &\quad - k e^{-L/\xi} (e^{-2/\xi} - 1). \end{aligned} \quad (28)$$

and when $L \gg \xi$ or $L \sim \xi$, above relation (28) is

$$\frac{E_g(L+2)}{L+2} - \frac{E_g(L)}{L} \sim -\frac{\pi}{6} \left(\frac{1}{(L+2)^2} - \frac{1}{L^2} \right) v c \quad (29)$$

Again considering Rt , for example, when $\xi = 2.0, v = 1.0, k = 1.0$, and $c = 1$, taking L/ξ on the horizontal axis, we obtain a relationship as shown in FIG. 9. This is consistent with the results of Sec.III-B.

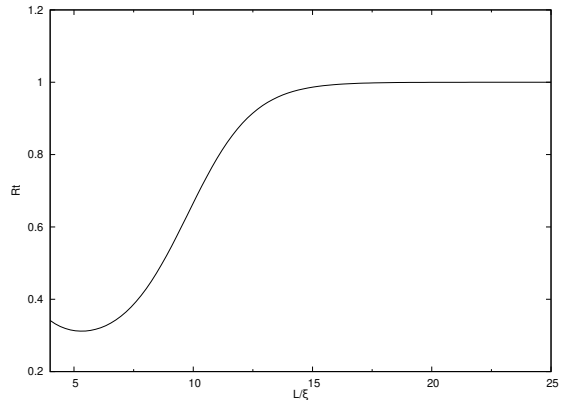


FIG. 9. example by eq.(28) : $\xi = 2.0, v = 1.0, k = 1.0, c = 1$

D. Massive case

In the off-critical regions such the Haldane and Néel phases, the correlation lengths are finite, thus the previous considerations do not hold. In this case, it is expected that the ground state energy behaves as

$$\frac{E_g(L)}{L} = \epsilon_\infty - A e^{-L/\xi(D)}. \quad (30)$$

where A is a constant and ξ is the correlation distance. In this case, $Rt \approx \exp(-2/\xi)$, thus off-critical behavior in FIG. 5 can be explained. This is also consistent with the results of Sec.III-B.

IV. DISCUSSIONS

In this section, we discuss symmetry aspects near the tetracritical point. And we compare previous research works with the present one.

A. Reinterpretation of Schulz's discussion

Reflecting on Schulz's work[1], he first rewrote the S=1 XXZ model (1) as the S=1/2 spin ladder system with ferromagnetic rung couplings.

Then, by using the bosonization method, he derived two independent effective field models. We consider that

the important point is the rung-inversion symmetry in the spin ladder system as shown in FIG. 10, which survives after approximations.

Thus eigenstates are divided into a rung-inversion symmetric sector and an antisymmetric sector. With this symmetry the four phases can intersect at one-point. Note that this rung-inversion symmetry is also important in the proof of Kitazawa et al[3].

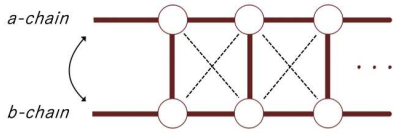


FIG. 10. The rung-inversion symmetry

B. Gibbs's phase rule

In general, for two intensive variables, it is known that the Gibbs's phase rule holds

$$F = C - P + 2, \quad (31)$$

where F is the number of degrees freedom, C is the number of components, and P is the number of phases.

In our cases, there exist two independent components as explained in Sec. IV-A, thus for four phases we obtain $F = 0$, which means a point.

C. Symmetry and universality

We discuss the difference between the symmetry of $D = 0$ in (4) and that of $\Delta = 0$ in (1). On the line $D = 0$ in (4), the model has an $SO(3)$ symmetry, thus the universality at the TB point is explained as the $SO(3)_1$ or the $SU(2)_2$ Wess-Zumino-Witten (WZW) model [13] with central charge $c = 3/2$. In the $SO(3)_1$ WZW model, there are several relevant fields, the important one of them has scaling dimension $x = 1$ with $SO(3)$ and translational invariance. Relaxing the symmetry to $SO(2)$, there exists another scaling field, and these two fields $x = 1$ explain the tetracritical behavior near the TB point.

Returning to the model (1), on the line $\Delta = 0$ it has the special $SU(2)$ symmetry as shown in (2) and (3). Nonetheless it should be noted that the special $SU(2)$ symmetry in the magnetization m even sector and that in the m odd sector are independent [3] (more precisely, this symmetry depends on boundary conditions; for open boundary condition, the special $SU(2)$ symmetry simply holds; for periodic boundary condition, one should extend twisted boundary conditions.). The special $SU(2)$ symmetry in the even m sector induces the $SU(2)_1$ WZW model with $c = 1$, or the BKT phase boundary. About the special $SU(2)$ symmetry in the odd m sector, it may be related with a different phase transition at the tetracritical point.

D. Previous numerical methods for XY1 - XY2 boundary.

At the Haldane-Néel phase boundary, the phenomenological renormalization group (PRG)[9] is valid because this is a second-order phase transition of order-disorder, which is a well established method[2].

For the XY1-XY2 phase boundary, the following magnetization-based methods have been used. The difference between the excitation energy and the ground energy is denoted by $\Delta E(m) = E(m) - E_g$.

Then we can define,

$$mrt \equiv \frac{\Delta E(m=2)}{\Delta E(m=1)} \quad (32)$$

From Schulz's discussion [1] and CFT, one can derive that $mrt = 4$ in XY1 phase and $mrt = 0$ in XY2 phase. Thus, numerically in [2] they used $mrt = 1$ to determine XY1-XY2 phases, whereas in [10], they used $mrt = 2$.

One cannot say whether method [2] or [10] is more suitable to determine the phase boundary. In fact, both methods can not be justified directly from Schulz's study [1].

Note that the jump of mrt may be used to detect XY1-XY2 phase boundary, this may not be related with the Haldane-Néel phase boundary.

E. Different CFT velocities

In eq.(19) of Sec. III-B, we have discussed that there may be two different CFT velocities. Such phenomena have been known in the spin-charge separation of the 1D Hubbard model[23, 24], which is Bethe-Ansatz solvable. In the case of less than half filling, both charge and spin excitations are gapless, and they are described as two $c = 1$ CFT with different velocities v_c, v_s .

For the spin chain case, such phenomena have not been studied, as far as we know.

V. CONCLUSION

In this paper, we have studied the S=1 XXZ spin chain with single ion anisotropy, and proposed a unified numerical method to determine the XY1-XY2 phase boundary and the Haldane-Néel phase boundary. These two phase boundaries continuously connect, thus combining with the BKT line already known on the $\Delta = 0$, there is a tetracritical point as expected in [1]. In addition, the XY1-XY2 phase boundary and the Haldane-Néel phase boundary are smoothly connected(i.e., differential is also continuous).

On the universality class of the tetracritical point, from the effective central charge, we discussed that this consists of the two independent field theories with different spin wave velocities. They can be explained with the rung inversion symmetry of the two leg spin ladder.

ACKNOWLEDGMENTS

We are grateful to K. Okamoto for discussions on this work. About the spin nematic phase, K. N. are taught from T. Momoi. We thank H. Katsura for references regarding the Takhtajan-Babujian point. K. N. is supported by Japan Society for the promotion of Science KAKENHI, GRANT No. 21H05021. S.S would like to acknowledge the support of the Kyushu University Leading Human Resources Development Fellowship Program. The numerical diagonalization program used in this study is based on the program developed by S.Moriya from TiTpack and Kobe Pack.

Appendix A: Perturbation theory and effective hamiltonian

Using ladder operators $S_i^\pm = S_i^x \pm iS_i^y$, Hamiltonian (1) is shown as

$$H = \sum_j \left(\frac{1}{2} (S_j^+ S_{j+1}^- + S_j^- S_{j+1}^+) + \Delta S_j^z S_{j+1}^z + D(S_j^z)^2 \right). \quad (\text{A1})$$

Denote the basis of the state space of the j th particle as

$$|\uparrow\rangle = \begin{pmatrix} 1 \\ 0 \\ 0 \end{pmatrix}, \quad |0\rangle = \begin{pmatrix} 0 \\ 1 \\ 0 \end{pmatrix}, \quad |\downarrow\rangle = \begin{pmatrix} 0 \\ 0 \\ 1 \end{pmatrix}, \quad (\text{A2})$$

so that, the representation matrix of the spin operators are

$$S^x = \frac{1}{\sqrt{2}} \begin{pmatrix} 0 & 1 & 0 \\ 1 & 0 & 1 \\ 0 & 1 & 0 \end{pmatrix}, \quad S^y = \frac{1}{\sqrt{2}} \begin{pmatrix} 0 & -i & 0 \\ i & 0 & -i \\ 0 & i & 0 \end{pmatrix}, \quad (\text{A3})$$

$$S^z = \begin{pmatrix} 1 & 0 & 0 \\ 0 & 0 & 0 \\ 0 & 0 & -1 \end{pmatrix}.$$

$$S^\pm = S^x \pm iS^y \quad (\text{A4})$$

For $D \rightarrow -\infty$, the terms not including D in Hamiltonian (A1) can be treated as a perturbation. Thus, we denote

$$H = D(S_j^z)^2 + \lambda V, \quad (\text{A5})$$

and the term containing V is considered a perturbation.

The eigenvalues of $D(S_j^z)^2$ for the j th site are 0 or D . When considering $D \rightarrow \infty$, D corresponds to the ground state energy. The eigenvalue D is doubly degenerate, with states $|\uparrow\rangle$ and $|\downarrow\rangle$. The entire system will have 2^N degeneracies for one eigenvalue ND .

When the j th $j+1$ th states are $|\uparrow\rangle$ and $|\downarrow\rangle$, respectively, and the state of the entire system is denoted as $|\uparrow_j \downarrow_{j+1}\rangle = |\uparrow_j\rangle \otimes |\downarrow_{j+1}\rangle$, then

$$|\uparrow_j \uparrow_{j+1}\rangle, |\uparrow_j \downarrow_{j+1}\rangle, |\downarrow_j \uparrow_{j+1}\rangle, |\downarrow_j \downarrow_{j+1}\rangle \quad (\text{A6})$$

have all the same eigenvalues. Here,

$$V = \sum_j (J_i (S_j^x S_{j+1}^x + S_j^y S_{j+1}^y) + \Delta S_j^z S_{j+1}^z) \quad (\text{A7})$$

is represented as $V = \sum_j V_j$, where $V_j = J_i (S_j^x S_{j+1}^x + S_j^y S_{j+1}^y) + \Delta S_j^z S_{j+1}^z$. Thus, we calculate $\langle \uparrow_j \uparrow_{j+1} | v | \uparrow_j \uparrow_{j+1} \rangle$ to obtain the matrix representation of v . However, since we are considering only the ground state, we can calculate the components of 2×2 matrix as follows. For example,

$$\begin{aligned} S_j^z S_{j+1}^z | \uparrow_j \uparrow_{j+1} \rangle &= \begin{pmatrix} 1 & 0 & 0 \\ 0 & 0 & 0 \\ 0 & 0 & -1 \end{pmatrix} \begin{pmatrix} 1 \\ 0 \\ 0 \end{pmatrix} \otimes \begin{pmatrix} 1 & 0 & 0 \\ 0 & 0 & 0 \\ 0 & 0 & -1 \end{pmatrix} \begin{pmatrix} 1 \\ 0 \\ 0 \end{pmatrix} \\ &= \begin{pmatrix} 1 \\ 0 \\ 0 \end{pmatrix} \otimes \begin{pmatrix} 1 \\ 0 \\ 0 \end{pmatrix} = | \uparrow_j \uparrow_{j+1} \rangle \end{aligned} \quad (\text{A8})$$

thus,

$$\langle \uparrow_j \uparrow_{j+1} | \Delta S_j^z S_{j+1}^z | \uparrow_j \uparrow_{j+1} \rangle = \Delta \quad (\text{A9})$$

Calculating the other components in the same way, the matrix representation of the Hamiltonian by perturbation of the first order $H_{eff}^{(1)}$ is

$$H_{eff}^{(1)} = \Delta \begin{pmatrix} 1 & 0 & 0 & 0 \\ 0 & -1 & 0 & 0 \\ 0 & 0 & -1 & 0 \\ 0 & 0 & 0 & 1 \end{pmatrix} \begin{matrix} | \uparrow \uparrow \rangle \\ | \uparrow \downarrow \rangle \\ | \downarrow \uparrow \rangle \\ | \downarrow \downarrow \rangle \end{matrix} \quad (\text{A10})$$

On the other hand, when $S = 1/2$, the matrix representation of the spin operator is

$$T^x = \frac{1}{2} \begin{pmatrix} 0 & 1 \\ 1 & 0 \end{pmatrix}, \quad T^y = \frac{1}{2} \begin{pmatrix} 0 & -i \\ i & 0 \end{pmatrix}, \quad T^z = \frac{1}{2} \begin{pmatrix} 1 & 0 \\ 0 & -1 \end{pmatrix}. \quad (\text{A11})$$

Thus, after simple calculations, we obtain

$$T_j^z T_{j+1}^z = \frac{1}{4} \begin{pmatrix} 1 & 0 & 0 & 0 \\ 0 & -1 & 0 & 0 \\ 0 & 0 & -1 & 0 \\ 0 & 0 & 0 & 1 \end{pmatrix} \begin{matrix} | \uparrow \uparrow \rangle \\ | \uparrow \downarrow \rangle \\ | \downarrow \uparrow \rangle \\ | \downarrow \downarrow \rangle \end{matrix} \quad (\text{A12})$$

If we map the $S=1$ state space to the $S=1/2$ state space, we can express the effective Hamiltonian as

$$H_{eff}^{(1)} = 4\Delta \sum_j T_j^z T_{j+1}^z, \quad (\text{A13})$$

using the expression $S=1/2$. Furthermore, let us consider second-order perturbations. Since the states that can transition are limited if we consider the selection rule, we only need to consider the case where the intermediate state is $|00\rangle$.

Calculating for each term,

$$\frac{\langle \uparrow_j \downarrow_{j+1} | \frac{1}{2} S_j^+ S_{j+1}^- | 00 \rangle \langle 00 | \frac{1}{2} S_j^+ S_{j+1}^- | \downarrow_j \uparrow_{j+1} \rangle}{-2D} = \frac{1}{-2D} \quad (\text{A14})$$

$$\frac{\langle \uparrow_j \downarrow_{j+1} | \frac{1}{2} S_j^+ S_{j+1}^- | 00 \rangle \langle 00 | \frac{1}{2} S_j^+ S_{j+1}^- | \uparrow_j \downarrow_{j+1} \rangle}{-2D} = \frac{1}{-2D} \quad (\text{A15})$$

$$\frac{\langle \downarrow_j \uparrow_{j+1} | \frac{1}{2} S_j^+ S_{j+1}^- | 00 \rangle \langle 00 | \frac{1}{2} S_j^+ S_{j+1}^- | \uparrow_j \downarrow_{j+1} \rangle}{-2D} = \frac{1}{-2D} \quad (\text{A16})$$

$$\frac{\langle \downarrow_j \uparrow_{j+1} | \frac{1}{2} S_j^+ S_{j+1}^- | 00 \rangle \langle 00 | \frac{1}{2} S_j^+ S_{j+1}^- | \downarrow_j \uparrow_{j+1} \rangle}{-2D} = \frac{1}{-2D} \quad (\text{A17})$$

we find that all these others are zero, therefore the Hamiltonian of the second-order perturbation $H_{eff}^{(2)}$ is

$$H_{eff}^{(2)} = \frac{1}{2|D|} \begin{pmatrix} 0 & 0 & 0 & 0 \\ 0 & -1 & -1 & 0 \\ 0 & -1 & -1 & 0 \\ 0 & 0 & 0 & 0 \end{pmatrix} \begin{matrix} | \uparrow \uparrow \rangle \\ | \uparrow \downarrow \rangle \\ | \downarrow \uparrow \rangle \\ | \downarrow \downarrow \rangle \end{matrix} \quad (\text{A18})$$

Further transforming, we obtain

$$H_{eff}^{(2)} = -\frac{1}{4|D|} \begin{pmatrix} 1 & 0 & 0 & 0 \\ 0 & 1 & 0 & 0 \\ 0 & 0 & 1 & 0 \\ 0 & 0 & 0 & 1 \end{pmatrix} + \frac{1}{4|D|} \begin{pmatrix} 1 & 0 & 0 & 0 \\ 0 & -1 & -2 & 0 \\ 0 & -2 & -1 & 0 \\ 0 & 0 & 0 & 1 \end{pmatrix} \quad (\text{A19})$$

where, the 1st term is constant.

Here again, for the $S = 1/2$ case, the matrix representation of the XXZ model is shown in

$$\frac{1}{2} J (T_j^+ T_{j+1}^- + T_j^- T_{j+1}^+) + J_z T_j^z T_{j+1}^z = \begin{pmatrix} \frac{1}{4} J_z & 0 & 0 & 0 \\ 0 & -\frac{1}{4} J_z & \frac{1}{2} J & 0 \\ 0 & \frac{1}{2} J & -\frac{1}{4} J_z & 0 \\ 0 & 0 & 0 & \frac{1}{4} J_z \end{pmatrix} \begin{matrix} | \uparrow \uparrow \rangle \\ | \uparrow \downarrow \rangle \\ | \downarrow \uparrow \rangle \\ | \downarrow \downarrow \rangle \end{matrix} \quad (\text{A20})$$

Comparing with the second term of equation (A19), we can put

$$J_z = \frac{1}{|D|}, \quad J = -\frac{1}{|D|} \quad (\text{A21})$$

Thus, in the second-order perturbation,

$$H_{eff}^{(2)} = \sum_j \left(-\frac{1}{|D|} (T_j^x T_{j+1}^x + T_j^y T_{j+1}^y) + \frac{1}{|D|} T_j^z T_{j+1}^z \right) \quad (\text{A22})$$

From (A13) and (A22), we obtain

$$H_{eff} = \sum_j \left(-\frac{1}{|D|} (T_j^x T_{j+1}^x + T_j^y T_{j+1}^y) + \left(\frac{1}{|D|} + 4\Delta \right) T_j^z T_{j+1}^z \right) \quad (\text{A23})$$

Furthermore, performing unitary transformations such as

$$T_j^{x,y} \rightarrow \begin{cases} -T_j^{x,y} & : j = 2i \\ T_j^{x,y} & : j = 2i + 1 \end{cases} \quad (\text{A24})$$

we obtain the $S=1/2$ XXZ model

$$H_{eff} = \sum_j \left(\frac{1}{|D|} (T_j^x T_{j+1}^x + T_j^y T_{j+1}^y) + \left(\frac{1}{|D|} + 4\Delta \right) T_j^z T_{j+1}^z \right) \quad (\text{A25})$$

whose properties are well known.

-
- [1] H. J. Schulz: Phys. Rev. B **34**, 6372 (1986)
- [2] W. Chen, K. Hida and B. C. Sanctuary: Phys Rev. B **67**, 104401 (2003)
- [3] A. Kitazawa, K. Hijii, and K. Nomura: J. Phys. A **36**, L351,(2003)
- [4] K. Nomura: J. Phys. A **28**, 5451, (1995)
- [5] K. Nomura and A. Kitazawa: J. Phys. A **31**, 7341, (1998)
- [6] A. Kitazawa: J. Phys. A, **30**, L285, (1997)
- [7] J. Solyom and T. Ziman: Phys. Rev. B **30**, 3980 (1984)
- [8] H. J. Schulz and T. Ziman: Phys. Rev, B **33**, 6545 (1986)
- [9] M. E. Fisher and M. N. Barber: Phys. Rev. Lett. **28**, 1516 (1972)
- [10] T.Tonegawa,K.Okamoto,K.Nomura,and T.Sakai: JPS Conf. Proc. **38**, 011154, 6 (2023)
- [11] L. A. Takhtajan: Phys. Lett. A **87**, 479 (1982).
- [12] H. M. Babujian: Phys. Lett. A **90**, 479 (1982); Nucl. Phys. B **215**, 317 (1983).
- [13] I. Affleck and F. D. M. Haldane: Phys. Rev. B **36**, 5291 (1987).
- [14] A. M. Tsvelick: Phys. Rev. B **42**, 10499 (1990)
- [15] G. De Chiara, M. Lewenstein and A. Sanpera: Phys. Rev. B **84**, 054451 (2011).
- [16] L. Lepri, G. De Chiara, and A. Sanpera: Phys. Rev. B **87**, 235107 (2013).
- [17] P. H. Ginsparg:“Applied Conformal Field Theory”, arXiv:hep-th/9108028.
- [18] A. Kitazawa and K. Nomura: JPSJ. A **66**, p.3944, (1997)
- [19] H. W. J. Blöte, J. L. Cardy and M. P. Nightingale: Phys.Rev. Lett. **56** 742 ,(1986).
- [20] I. Affleck: Phys. Rev. Lett. **56**, 746 (1986).
- [21] J. L. Cardy: Nucl. Phys. B **270** [FS16], 186 (1986).
- [22] P. Reinicke: J. Phys. A: Math. Gen. **20**, 5325 (1987).
- [23] F. Woynarovich: J. Phys. A **22**, 4243 (1989).
- [24] H. Frahm and V. E. Korepin: Phys. Rev. B **42**, 10553 (1990).